Human iPSC-derived microglia assume a primary microglia-like state after transplantation into the neonatal mouse brain

Devon S. Svoboda[a], M. Inmaculada Barrasa[a,b], Jian Shu[a,c], Rosalie Rietjens[a], Shupei Zhang[a], Maya Mitalipova[a], Peter Berube[c], Dongdong Fu[a], Leonard D. Shultz[d], George W. Bell[a,b], and Rudolf Jaenisch[a,e,1]

[a]Whitehead Institute for Biomedical Research, Cambridge, MA 02142; [b]Bioinformatics and Research Computing, Whitehead Institute for Biomedical Research, Cambridge, MA 02142; [c]Broad Institute of MIT and Harvard, Cambridge, MA 02142; [d]The Jackson Laboratory Cancer Center, The Jackson Laboratory, Bar Harbor, ME 04609; and [e]Department of Biology, Massachusetts Institute of Technology, Cambridge, MA 02142

Contributed by Rudolf Jaenisch, October 16, 2019 (sent for review August 8, 2019; reviewed by Valentina Fossati and Helmut Kettenmann)

Microglia are essential for maintenance of normal brain function, with dysregulation contributing to numerous neurological diseases. Protocols have been developed to derive microglia-like cells from human induced pluripotent stem cells (hiPSCs). However, primary microglia display major differences in morphology and gene expression when grown in culture, including down-regulation of signature microglial genes. Thus, in vitro differentiated microglia may not accurately represent resting primary microglia. To address this issue, we transplanted microglial precursors derived in vitro from hiPSCs into neonatal mouse brains and found that the cells acquired characteristic microglial morphology and gene expression signatures that closely resembled primary human microglia. Single-cell RNA-sequencing analysis of transplanted microglia showed similar cellular heterogeneity as primary human cells. Thus, hiPSCs-derived microglia transplanted into the neonatal mouse brain assume a phenotype and gene expression signature resembling that of resting microglia residing in the human brain, making chimeras a superior tool to study microglia in human disease.

microglia | chimera | P2RY12 | RNA-seq | CSF1

Microglia are the resident immune cells of the brain and fulfill a number of crucial functions, including immune surveillance (1), sculpting neural circuits through synaptic pruning (2), and clearing protein debris (3, 4). In addition, impaired microglial function is thought to contribute to a variety of neurological and neurodegenerative diseases, including Alzheimer's and Parkinson's diseases (5–7). Increased microglial activation has been observed in both patients and mouse models of neurodegenerative diseases, and this increased activation is hypothesized to contribute to neuronal dysfunction and death (8–11). In addition, multiple GWAS studies searching for loci associated with increased risk for neurodegenerative disease have identified genes which are highly expressed in microglia, including *APOE* and *TREM2* (12–17). These discoveries identify microglial function as a key factor contributing to the development of Alzheimer's and Parkinson's diseases.

The recent development of protocols to differentiate induced microglia-like cells (iMGs) from human induced pluripotent stem cells (hiPSCs) has provided the opportunity to study these cells in vitro under defined culture conditions (18–23). The success of these protocols lies in mimicking in vivo microglial development in an in vitro setting. Stem cells are first induced to a hematopoietic lineage and then into myeloid intermediates, similar to primitive macrophages (18, 20–23) or monocytes (19). As microglial differentiation in vivo is driven primarily by cytokines secreted from neurons and astrocytes (including IL34, MCSF1, and CX3CL1) (24, 25), microglial differentiation in vitro is achieved either by addition of these cytokines to the media to mimic the presence of neurons (18, 19, 21) or by growing microglia in co-culture with neural cells (20, 22, 23).

Despite these innovations, there are important limitations to modeling human disease with hiPSC-derived iMGs. As immune cells, microglia are prone to activation and highly sensitive to in vitro culture, which introduces impediments in extending results obtained with cultured cells to disease states. This is highlighted by recent studies showing that primary microglia directly isolated from the brain exhibit significant changes in gene expression when grown in culture for as little as 6 h (26, 27). These changes include down-regulation of key microglial genes such as *TMEM119* and *P2RY12*, and up-regulation of genes associated with microglial activation or disease states (26, 27). Thus, the available evidence indicates that the phenotype and gene expression signature of in vitro cultured microglia are significantly different from that of primary, resting microglia in the brain.

To address these issues, several studies have attempted transplantation of mouse (20, 23) or human (18) iPSC-derived microglia-like cells into adult (18, 20) or neonatal (23) mouse brains. Although these studies did show successful integration of small numbers of cells with branched morphology, they lack the sufficient numbers of transplanted cells to do further characterization or manipulation, and fail to compare the transplanted

Significance

Microglia, the resident immune cells of the brain, are known to be crucial for normal brain function as well as contributing to neurodegenerative disease. However, microglial cells are very sensitive to culture conditions and have been shown to lose their key properties when grown in vitro. In this study, we developed a model in which we transplant immature microglial cells derived from human stem cells into the brains of neonatal mice. By growing microglia in the environment of the mouse brain, the stem cell-derived microglial cells acquire key aspects of microglial morphology and gene expression which cannot be attained in culture, and are therefore a better representation of human microglial cells for the purpose of studying human disease.

Author contributions: D.S.S. and R.J. designed research; D.S.S., J.S., R.R., P.B., and D.F. performed research; M.M. and L.D.S. contributed new reagents/analytic tools; D.S.S., M.I.B., R.R., S.Z., and G.W.B. analyzed data; and D.S.S. and R.J. wrote the paper.

Reviewers: V.F., New York Stem Cell Foundation; and H.K., Max Delbrück Center for Molecular Medicine.

The authors declare no competing interest.

Data deposition: The single-cell and bulk RNA-sequencing data reported in this paper have been deposited in the Gene Expression Omnibus (GEO) database, https://www.ncbi.nlm.nih.gov/geo (accession no. GSE139194).

[1]To whom correspondence may be addressed. Email: jaenisch@wi.mit.edu.

This article contains supporting information online at https://www.pnas.org/lookup/suppl/doi:10.1073/pnas.1913541116/-/DCSupplemental.

First published November 26, 2019.

cells with primary human microglia to confirm that in vivo differentiation was successful.

To establish an experimental platform to allow the generation of hiPSC-derived microglia that resemble primary microglia, induced human microglia (iMGs) were transplanted into the brains of neonatal mice expressing human CSF1. Two months after transplantation, the cells assumed a phenotype and gene expression signature that were more similar to that of primary microglia directly isolated from the human brain than to primary microglia cultured for 7 d. Compared with in vitro differentiated microglia, the transplanted iMGs expressed higher levels of key microglial signature genes and more closely resembled primary microglia residing in the human brain. Our results show that the human–mouse microglial chimera is a powerful tool for the study of human microglia in health and disease.

Results

Generation of Human–Mouse Microglial Chimeras. Multiple protocols have been established to generate microglia-like cells from human embryonic stem cells or hiPSCs (18–23). These in vitro cultured cells exhibited significant morphological differences compared with primary human microglia, suggesting that in vitro culture may fundamentally change microglial physiology (18–23). The goal of this study was to investigate how the in vivo environment would affect the microglial phenotype by transplanting in vitro derived human microglia into the neonatal mouse brain. To make human–mouse microglial chimeras, stem cells were differentiated into microglial precursors (iMPs) (19, 28) at a high purity of a minimum of 98% CD11b+CD45+ cells (Fig. 1 *A* and *B*) using an established protocol (19). These iMPs were then transplanted to create chimeric mice or plated for in vitro microglial differentiation. Following 2 wk of in vitro microglial differentiation, expression of microglial markers increased or was maintained relative to microglial precursors (*SI Appendix*, Fig. S1). To detect the presence of human cells in the brains of the mouse recipients, donor cells carried a green fluorescent protein (GFP) reporter (*SI Appendix*, Fig. S2).

Growth and survival of microglia depend on CSF1 and other cytokines (24, 29, 30). Because human myeloid cells do not respond efficiently to murine cytokines, mice carrying transgenes encoding human *CSF1*, *IL3*, *SCF*, and *GM-CSF* were derived and have been shown to better support the survival of transplanted human cells into the hematopoietic compartment (31–33). To assess whether these human cytokines improved the integration and differentiation of human microglial precursors into microglia, we transplanted hiPSC-derived iMPs into the brains of NOD scid gamma (NSG) mice and NSG mice carrying the human transgenes encoding *IL3*, *SCF*, and *GM-CSF* (NSG-Triples; NSG-T) or, in addition, also carrying the human version of *CSF1* (NSG-Quads; NSG-Q) (Fig. 1*A*). When iMPs were transplanted, immunohistochemical analysis revealed robust integration and survival of GFP+ cells in NSG-Quads (Fig. 1*C1*). The average number of GFP+ cells increased from over 2,500 cells per 100-μm-thick brain section at 10 d post injection (dpi) (Fig. 1*C2*) to 6,900 cells per section at 60 dpi (Fig. 1*C3*), and then to 15,000 GFP+ cells per section at 120 dpi (Fig. 1 *C1* and *C4*). In contrast, very few GFP+ cells remained after 10 dpi in NSG-T or NSG hosts (Fig. 1 *C1* and *C5* and *SI Appendix*, Fig. S3*C*), indicating that human *IL3*, *SCF*, and *GM-CSF* are not sufficient to support transplanted iMPs in the mouse brain. Thus, human *CSF1* is crucial for the survival and integration of transplanted human iMPs in chimeric mouse brains.

Previous studies have shown the importance of matching the developmental state of transplanted cells to the recipient host (34, 35). To determine whether a precursor or a differentiated microglial cell is better matched for transplantation into neonatal mouse brains, we injected iMPs, or iMPs differentiated for 1 or 2 wk into microglia-like cells, into the lateral ventricles of P1 neonatal NSG-T and NSG-Q mice (Fig. 1*A*). Chimeras generated from the injection of iMPs had high numbers of GFP+ cells at 10 and 60 dpi (2,500 and 6,900 cells per section, respectively). In contrast, chimeras injected with microglia-like cells differentiated in vitro for 2 wk had significantly fewer GFP+ cells per section (*SI Appendix*, Fig. S3 *A* and *B*), with an average of 270 cells per section at 10 dpi and 1,080 cells per section at 60 dpi. Injection of microglia-like cells differentiated 1 wk in vitro was similar to injection of iMPs at 30 dpi (*SI Appendix*, Fig. S3 *D* and *E*). Thus, we conclude that iMPs more efficiently integrate into the brains of neonatal mice than the in vitro differentiated microglia-like cells. Furthermore, these results emphasize the necessity of utilizing an in vitro differentiation protocol that includes a time point at which precursor cells can be collected at high purity to generate microglial chimeras.

By 10 dpi, GFP+ cells in NSG-Q mice had migrated away from the site of injection and were spreading throughout the striatum and cortex, indicating successful integration into the host tissue (Fig. 1 *C2* and *D*). The GFP+ cells within the brain tissue were ramified and displayed characteristic microglial morphology (Fig. 1*D*), again suggesting integration of the GFP+ human cells into the environment of the murine brain. Rounded, unramified GFP+ cells were attached to the meninges surrounding the outside of the brain and within the folds of the cerebellum (Fig. 1*C*). These cells were ∼20% of GFP+ cells in the entire section anterior to the cerebellum at 10 dpi and 5% at 120 dpi (*SI Appendix*, Fig. S3*F*). GFP+ cells were confirmed to be human cells through labeling with an antibody against human nuclei (Fig. 1*D1*), and were shown to maintain expression of Pu.1 and Iba1, which are markers of the myeloid lineage (Fig. 1*D2*).

Human microglia were unevenly distributed in the brain, with the highest contribution of GFP+ cells in the olfactory bulb and striatum at 120 dpi (Fig. 1*C4*). To assess the fraction of human cells in the overall microglial population, we determined the fraction of GFP+ cells in the Pu.1+ cell population, which encompasses both human and mouse microglia. Human cells made up a significant percentage of the total microglia, with 27% of all microglia being GFP+ in the whole brain anterior to the cerebellum (calculated as %GFP/Pu.1). In structures with the highest contribution of human cells such as the caudate, up to 50% of microglia were found to be GFP+ (Fig. 1*E*). We observed an increase in the total number of Pu.1+ cells in anatomical regions with high integration of GFP+ iMGs, with no decrease in the number of GFP-negative, Pu.1+ mouse microglia (*SI Appendix*, Fig. S3*G*) in NSG-Q chimeras relative to NSG-T controls, which did not have transplanted cells remaining. Thus, the invasion of human donor cells into the different brain regions did not reduce the number of mouse microglia.

Transplanted Microglial Precursors Mature into Microglia. To confirm that the transplanted iMPs had adopted a microglial identity within the environment of the mouse brain, cells were stained for expression of the microglial specific markers P2RY12 and TMEM119. At 10 dpi, 40 to 60% of GFP+ cells with microglial morphology colabeled with P2RY12 in the cortex and striatum, respectively, while greater than 95% of cells expressed myeloid marker Iba1 (Fig. 2 *A* and *B*). However, no P2RY12 staining was detected in the unramified cells located in the meninges at the edge of the brain, even though expression of Iba1 remained at 91% (Fig. 2 *A* and *B*), suggesting that these cells, while myeloid, had not matured into microglia. At 60 dpi, over 99% of GFP+ cells colabeled with both P2RY12 and Iba1 (Fig. 2 *B* and *C*) in the striatum and cortex. In contrast, while 83% of unramified cells in the meninges expressed Iba1 at 60 dpi, only 3% expressed P2RY12 (Fig. 2 *B* and *C*). TMEM119, another developmentally regulated microglial specific marker (36), was robustly expressed at 60 dpi but below the level of detection at 10 dpi (Fig. 2*D*). The fraction of transplanted cells expressing P2RY12 increased

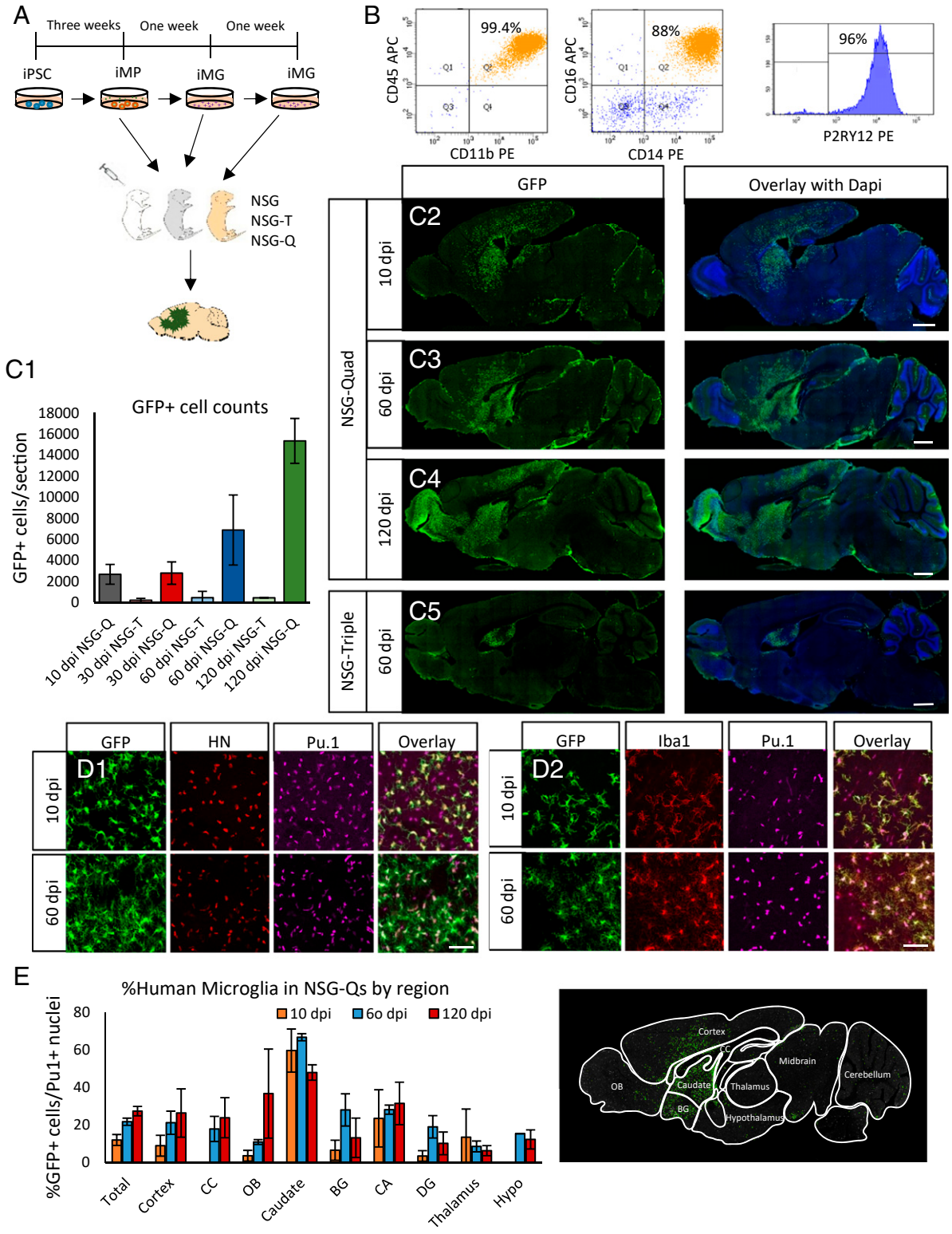

Fig. 1. Generating human–mouse microglial chimeras. (*A*) iPSCs were differentiated into microglial precursors (19) and further differentiated in vitro into microglia for 1 or 2 wk (*Materials and Methods*). iMPs and iMGs were injected into neonatal NSG mice with a transgene encoding human alleles for *CSF1*, *SCF*, *IL3*, and *GM-CSF* (NSG-Q) or *SCF*, *IL3*, and *GM-CSF* (NSG-T) or no human alleles (NSG). Mice were taken at 10, 30, 60, or 120 d post injection. Image of neonates from UNSW Embryology (https://embryology.med.unsw.edu.au) and image of mouse brain from Wikimedia Commons (https://commons.wikimedia.org/wiki/File:Mouse_brain_sagittal.svg). (*B*) FACS analysis of iMPs used for transplantation shows cells are 99% CD11b+CD45+, 88% CD14+CD16+, and 96% P2RY12+ in a representative experiment. (*C*) Quantification of the number of GFP+ cells per 100-μm-thick section at various time points of NSG-Q and NSG-T chimeras (*C1*). Values are expressed as mean ± SD. Representative images of NSG-Q chimera brains at 10 dpi (*C2*), 60 dpi (*C3*), and 120 dpi (*C4*), as well as NSG-T at 60 dpi (*C5*). (Scale bars, 1,000 μm.) (*D*) Higher-magnification images of GFP+ cells at 10 and 60 dpi, colabeled with markers of human nuclei (red) and Pu.1 (purple) (*D1*) as well as myeloid lineage Iba1 (red) and Pu.1 (purple) (*D2*). (Scale bars, 50 μm.) (*E*) Percentage of total microglia that are of human origin, expressed as %(GFP+ cells)/(Pu.1+ cells), is shown for the entire section and for selected brain regions at 10, 60, and 120 dpi. Values are expressed as mean ± SD. Anatomical regions drawn on a representative section are shown (*Right*). BG, basal ganglia; CA, cornu ammonis; CC, corpus callosum; DG, dentate gyrus; Hypo, hypothalamus; OB, olfactory bulb.

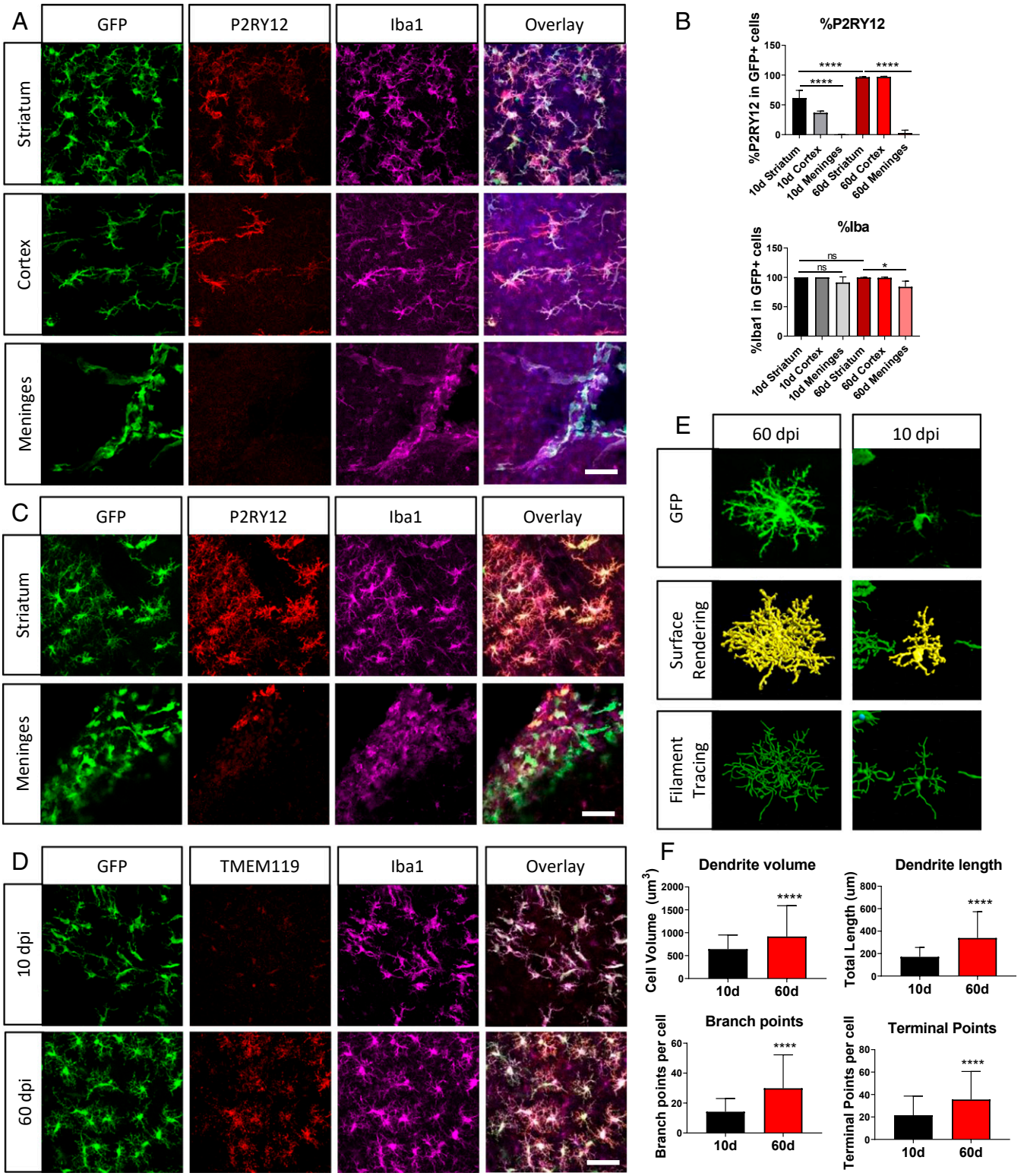

Fig. 2. Transplanted microglial precursors differentiate and mature into microglial cells in vivo. (*A*) At 10 dpi, GFP+ cells are shown from the striatum, cortex, and meninges. (Scale bar, 50 μm.) (*B*) The percentages of GFP+ cells that colabel with P2RY12 (*Top*) and Iba1 (*Bottom*) are quantified in the striatum, cortex, and meninges at 10 and 60 dpi. Values are expressed as mean ± SD. Significance was determined with one-way ANOVA with Tukey post hoc test, with sample sizes of 3 mice per group. (*C*) At 60 dpi, GFP+ cells are shown in the striatum and meninges. (Scale bar, 50 μm.) (*D*) Representative images of transplanted GFP+ cells at 10 dpi (*Top*) and 60 dpi (*Bottom*) colabeled with TMEM119 (red). (Scale bar, 50 μm.) (*E*) GFP+ iMGs increase in complexity from 10 to 60 dpi. Representative cells are depicted as fluorescent images showing GFP expression (*Top*), a surface rendering (*Middle*), and a filament tracing (*Bottom*). (*F*) From the filament tracings, the total length of all summed processes (dendrite length), total volume of all summed processes (dendrite volume), total number of bifurcation points (branch points), and total number of process terminal points (terminal points) were measured per cell at 10 and 60 dpi. Values are expressed as mean ± SD. Filament tracings and quantifications were performed in Imaris. Significance was determined with Mann–Whitney *t* test, with sample sizes of 150 to 300 cells from 3 mice. $*P < 0.05$, $****P < 0.001$; ns, not significant.

between day 10 and day 60, suggesting that the microglia were still immature at 10 dpi but matured to more definitive microglia at 60 dpi. Consistent with this possibility, transplanted iMGs developed into a typical morphological complexity between 10 and 60 dpi (Fig. 2*E*), with filament tracing of individual GFP+ cells showing an increase in the overall length and volume of the cell processes as well as an increase in the number of branch points and terminal points (Fig. 2*F*). These observations suggest that transplantation of human microglial precursors into the mouse brain represents a powerful system for studying the signals which induce the differentiation and maturation of microglia in an in vivo environment.

Human iMGs Residing in Rodent Brains Are Similar to Primary Human Microglia. Recent work has shown that primary microglia isolated from mouse (26) and human (27) brains show dramatic changes in gene expression following as little as 6 h in culture. We compared gene expression of iMGs directly isolated from the brains of transplanted NSG-Q neonates with cells differentiated in vitro to determine how the transcriptome of microglia changed after transplantation into the brain. We collected fluorescence-activated cell sorting (FACS)-sorted GFP+ cells from chimeric brains at 0 dpi (i.e., the cells used for transplantation), 10 dpi, and 60 dpi as well as iMGs cultured in vitro for the same time period and performed bulk RNA sequencing (RNA-seq). Using principal-component analysis (PCA), in vivo differentiated samples clustered separately from in vitro differentiated samples at 10 and 60 dpi (Fig. 3*A1*), indicating that transplantation into the brain changed the transcriptome of iMGs. In vivo differentiated iMGs isolated at 10 dpi clustered closer to iMPs than to iMGs isolated at 60 dpi, which suggests a developmental progression after transplantation (Fig. 3*A1*). In contrast, iMGs differentiated in vitro for 10 and 60 d clustered close together, consistent with little or no maturation occurring after prolonged in vitro culture. In vitro iMGs and 10-dpi in vivo iMGs clustered at similar positions along the *y* axis of the PCA plot (PC2) (Fig. 3*A1*), indicating some similarities in gene expression.

To correlate gene expression of iMGs transplanted into the brain with that of primary human microglia, we compared isolated in vivo iMG samples with gene expression of microglia directly isolated from human brain or after in vitro culture for 7 d (27). Following batch correction using Combat to remove differences in gene expression due to technical effects, in vivo transplanted iMGs appeared to cluster much more closely to primary human microglia (MGs) than in vitro differentiated iMGs, especially at 60 dpi (Fig. 3*A2*). Likewise, in vitro differentiated iMGs clustered more closely to primary human MGs which had been cultured in vitro for 7 d. In order to quantify the relative distances of the separate samples to primary human MGs, the distance between each sample and the center of the primary human MG was measured (Fig. 3*A3*), and 60-dpi in vivo iMGs were found to be significantly closer to primary human microglia than all other samples tested. Thus, the 60-dpi in vivo iMGs were found to be more similar to primary human MGs than with in vitro cultured microglia.

To further define gene expression differences between different in vivo and in vitro microglia, we performed scatterplots of log-transformed gene counts between all sample pairs (Fig. 3*B* and *SI Appendix*, Fig. S4). Comparisons were done using all genes as well as a list of microglial signature genes generated by Gosselin et al. (27). Using both gene sets, comparisons between 60-dpi in vivo iMGs and primary microglia resulted in higher R^2 values ($R^2 = 0.97$ for all genes; $R^2 = 0.89$ for microglial genes) than similar comparisons between 60-dpi in vivo iMGs and primary monocytes ($R^2 = 0.76$; $R^2 = 0.28$) (Fig. 3*B*). This is consistent with iMPs differentiating into microglia after injection into the neonatal mouse brain, rather than a different type of myeloid cell. In addition, 60-dpi in vivo iMGs also had higher R^2 values when compared with primary microglia than in vitro microglia ($R^2 = 0.89$; $R^2 = 0.58$). In contrast, 60-d in vitro iMGs had the highest R^2 values when compared with in vitro cultured microglia ($R^2 = 0.96$; $R^2 = 0.89$) than when compared with either primary microglia ($R^2 = 0.90$; $R^2 = 0.64$) or monocytes ($R^2 = 0.81$; $R^2 = 0.40$) (*SI Appendix*, Fig. S4*A*). In all cases, the differences between R^2 values were greater when comparisons were done using microglial enriched genes. Our results again suggest that iMGs differentiated in vivo are more similar to primary human microglia than in vitro differentiated iMGs.

To determine whether similar sets of genes were differentially expressed between in vitro and in vivo conditions in iMGs and primary microglia, we plotted all genes which were differentially expressed in either the current study or Gosselin et al. by the ratio of expression of in vivo samples compared with that of in vitro samples. Fig. 3*C* shows that far more genes changed in the same direction in both studies than in opposite directions ($P = 1e^{-300}$ by Fisher exact test), indicating that transplantation of iMGs into the brain creates cells that closely resemble primary human microglia.

Increased Expression of MG Signature Genes in Microglia after Transplantation into the Brain. Microglial differentiation is thought to be dependent on signals derived from neurons and astrocytes (24, 37). Indeed, microglial differentiation protocols use molecules like IL34 secreted by neurons to drive acquisition of a microglial phenotype (18–20, 24) which are thought to be necessary for the acquisition of microglial identity. To determine whether transplantation into the brain affected the expression of microglial signature genes, genes differentially expressed in 60-dpi transplanted in vivo iMGs and iMGs cultured in vitro for 60 d are shown in a volcano plot with labels for the 50 genes exhibiting the greatest *P* value (Fig. 3*D* and Dataset S1). In addition, a heatmap shows the expression of these differentially expressed genes across all samples, with labels of key microglial signature genes and disease risk genes (Fig. 3*E* and *SI Appendix*, Fig. S5*A*). Among the genes with dramatically increased in vivo expression are core microglial genes such as *P2RY12*, *P2RY13*, *CX3CR1*, *SALL1*, and *BIN1* (Fig. 3 *D–F* and *SI Appendix*, Fig. S5*B*), which mirrors changes in gene expression when primary human (27) and mouse (26) microglia were cultured. Gene ontology analysis of 2-fold up-regulated genes in transplanted iMGs at 60 dpi showed enrichment in terms related to immune function, including leukocyte differentiation, cytokine production, and B cell proliferation (*SI Appendix*, Table S1). In contrast, down-regulated genes were enriched for terms associated with immune activation, including myeloid leukocyte activation, leukocyte migration, cytokine production, and regulation of inflammatory response (*SI Appendix*, Table S1). Thus, transplanted iMGs exhibit patterns of gene expression which are consistent with increased expression of genes important for microglial identity and down-regulation of genes involved in the inflammatory response.

Microglia have been shown to be activated in different neurodegenerative diseases (5–7), and numerous Alzheimer's and Parkinson's disease risk loci have been mapped to genes with high expression in microglia (12–17). We found a significant increase in expression of disease-associated genes such as *GPNMB*, *ANXA1*, *APOC1*, and *SNCA* in cultured iMGs as compared with iMGs residing in the brain (Fig. 3*G* and *SI Appendix*, Fig. S5*C*). Thus, cultured iMGs may not be a faithful experimental system to assess gene expression changes related to neurodegenerative disease mechanisms.

iMGs Differentiated In Vitro Resemble Primary Human Microglia in a Diseased State. Microglia have recently been described as exhibiting heterogeneity in function and gene expression throughout

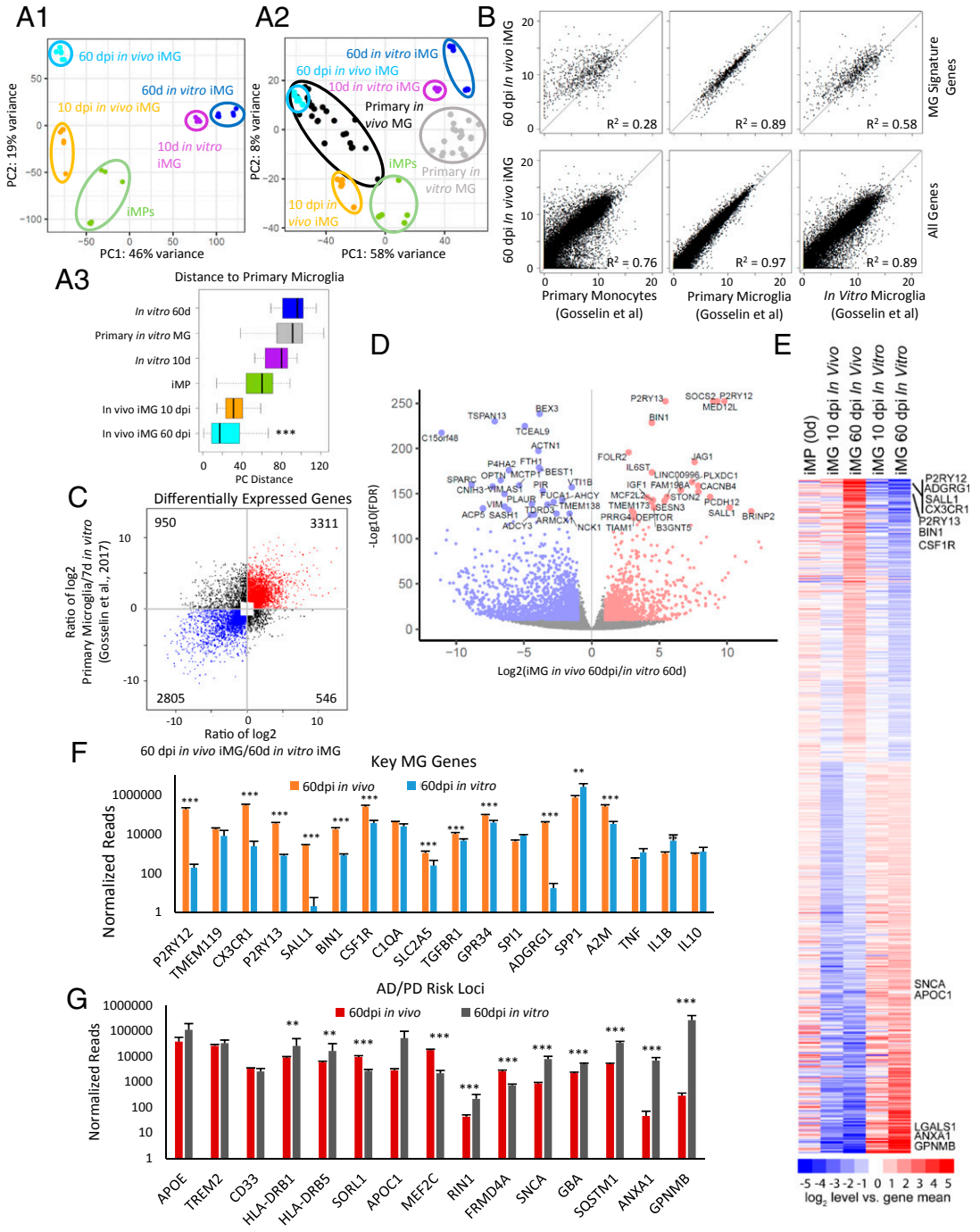

Fig. 3. iMGs differentiated in chimeric brains are more similar to primary microglia than iMGs differentiated in vitro. (*A1*) PCA depicting the variance in expression (normalized counts) of the best discriminating 500 features in iMPs (green), transplanted iMGs isolated from chimeras at 10 dpi (orange) and 60 dpi (light blue), and iMGs differentiated in vitro for 10 d (purple) and 60 d (dark blue). (*A2*) PCA of the above samples combined with previously published data from primary microglia immediately after isolation (black) and primary microglia following 7 d in culture (gray) (27). (*A3*) PCA Euclidean distances to the primary microglia samples were calculated between all pairs of points in each group, using PC1 and PC2 on the top 500 genes. Distances were compared using ANOVA, followed by Dunnett's test. (*B*) Log-transformed scatterplots comparing gene expression of 60-dpi in vivo iMGs with primary monocytes (*Left*), microglia (*Middle*), and primary microglia cultured for 7 d (*Right*) using microglial signature genes (*Top*) or all genes (*Bottom*). (*C*) Scatterplot comparing the ratio of log2-transformed normalized counts in 60-dpi in vivo iMGs/60-d in vitro iMGs (log2 fold change > 1; false discovery rate [FDR] < 1e-05) with the ratio of log2-transformed normalized counts in primary microglia/cultured microglia for differentially expressed genes. (*D*) Volcano plot of all genes detected, showing the ratio of expression between 60-dpi in vivo iMGs and 60-d in vitro iMGs. Gene expression is depicted as the ratio of log2-transformed normalized counts (*x* axis) by log10-transformed normalized counts (*y* axis). Colored genes are differentially expressed (FDR < 1e-10; fold change > 2), with blue dots indicating those that are higher in 60-d in vitro iMGs, and red dots indicating genes that are higher in 60-dpi in vivo iMGs. (*E*) Heatmap showing relative (mean-centered) gene expression across all samples. The map includes genes differentially expressed between in vivo and in vitro iMGs at 60 d, ordered by the ratio of those samples. (*F*) Expression of selected key microglial genes on a log10 scale in 60-dpi in vivo iMGs and 60-d in vitro iMGs. Values are expressed as normalized counts ± SD. (*G*) Expression of selected genes associated with risk loci for Alzheimer's disease (AD) or Parkinson's disease (PD) on a log10 scale in 60-dpi in vivo iMGs and 60-d in vitro iMGs. Values are expressed as normalized counts ± SD. $n = 6$ for all sample sets. $^{**}P < 0.001$, $^{***}P < 0.001$ or less.

development and in disease states in both human (38) and mouse (8, 39). To determine whether iMGs differentiated in chimeric brains exhibited similar heterogeneity, we compared gene expression from in vivo iMGs at 60 dpi with iMGs cultured in vitro for 60 d by single-cell RNA-seq (scRNA-seq). In addition, we compared the in vivo and in vitro differentiated iMG primary microglia from healthy donors and patients with multiple sclerosis (MS) (38). UMAP (uniform manifold approximation and projection) plots were generated showing 4 replicates of transplanted iMGs, 2 replicates of in vitro differentiated iMGs, primary microglia from healthy donors, and primary microglia from MS patients (Fig. 4*A*); all differentially expressed genes for individual clusters are listed in Dataset S2. This analysis generated 13 clusters, with in vivo iMGs predominantly located in clusters 1, 2, 3, and 4, healthy primary microglia located in clusters 1, 3, 5, and 7, in vitro iMGs located in clusters 0, 4, 6, and 8, and primary MS microglia located in clusters 0, 2, 9, and 10 (Fig. 4*B*). In particular, when the UMAP plot was colored according to samples (Fig. 4*A*, *Left*), distinct overlaps between transplanted iMGs and healthy primary microglia were observed as shown in the right panel of the graph, and clear overlap was seen between in vitro differentiated iMGs and microglia from MS patients on the left side of the plot. To quantify these observations, the UMAP distance was measured between each individual cell and the center of the region occupied by the healthy primary microglia (Fig. 4*C*). Using a Scheffé test, the transplanted iMGs were found to be significantly closer to the healthy primary microglia than were the in vitro and MS samples. These results confirm that the iMGs differentiated in the chimeric mouse brain are more similar to primary microglia than iMGs differentiated in vitro. Furthermore, these results suggest that iMGs differentiated in vitro resemble primary microglia in a disease state.

To evaluate the expression of microglial signature genes in the different clusters, we generated a microglial signature score that combined expression of key microglial genes (*TMEM119*, *P2RY12*, *P2RY13*, *CX3CR1*, *CSF1R*, and *BIN1*) and overlaid it on the UMAP plot, with each cell colored according to its expression of these genes (Fig. 4*D*). This indicated that cells in clusters containing primarily transplanted iMGs and healthy primary microglia have much higher microglial scores than cells in clusters containing primarily in vitro iMGs or MS microglia. In contrast, when we analyzed selected genes which are more generally expressed in all macrophage cell types (*AIF1*, *SPI1*, and *GPR34*), expression levels appeared much more consistent across clusters (Fig. 4*E*). Notably, cells in cluster 2, which is 87% in vivo iMGs and 13% MS microglia (Dataset S3), had low microglial signature scores compared with cluster 1 but normal expression of other myeloid genes such as AIF1 and SPI1. These cells could represent the nonmicroglial GFP+ macrophages on the edges of the chimeric brains and perivascular macrophages lining the blood vessels (Fig. 1 and *SI Appendix*, Fig. S3*H*), while clusters 1 and 3 represent the microglial iMGs found within the neuropil of the brain.

In our previous results, we found that some genes associated with neurodegenerative disease were up-regulated in the in vitro samples. To determine if this was recapitulated using scRNA-seq, we overlaid the expression level of *MARCO*, *LGALS1*, and *GPNMB* associated with Parkinson's disease on the UMAP plot (Fig. 4*F*). These genes had much higher expression in clusters containing primarily in vitro iMGs or MS microglia. A heatmap showing the 40 most differentially expressed genes in the largest clusters, clusters 0 through 5, is shown in Fig. 4*G*. The most differentially expressed genes in the remaining clusters are shown in *SI Appendix*, Fig. S6. These results further confirm that the iMGs grown in vitro have up-regulation of genes associated with disease states, while iMGs grown in the in vivo environment resemble resting primary microglia.

iMGs In Vivo Respond to Lipopolysaccharide Stimulation. Lipopolysaccharide (LPS) stimulation is a classic model of immune activation and the resulting microglial activation has been well-characterized in mice (36, 40, 41). This activation response includes a shift to a less ramified, amoeboid morphology and an increase in expression of cytokines such as TNF alpha and IL1 beta. To assess whether the iMGs responded to immune stimulation, 60-dpi chimeric mice were injected with LPS or saline and brains were collected for immunohistochemistry after 24 h. P2RY12+ iMGs in mice injected with saline showed extensive ramification similar to that already described (Fig. 5*A*, *Left*). In contrast, P2RY12+ iMGs in mice injected with LPS were less ramified and exhibited activated morphology (Fig. 5*A*, *Right*). Despite identical LPS injections, variability was observed in the degree of morphological changes between chimeras. Some chimeras showed cells with thickened, shorter processes with a complete loss of the fine, branching processes as seen in the control iMGs (Fig. 5*A*, *Middle*), while the more severely affected chimeras had iMGs with round amoeboid appearance (Fig. 5*A*, *Right*). Given that the reasons for this variability are unknown, cells from severely and moderately affected chimeras were pooled into a single group. Morphological quantification of iMGs in saline- and LPS-injected chimeras revealed significant decreases in total process length, volume, branch points, and terminal points (Fig. 5*B*), indicating that transplanted iMGs exhibit this key function of primary microglia. LPS stimulation is also known to increase phagocytosis in primary microglia (42, 43). To determine if transplanted iMGs functionally responded to LPS by increasing phagocytosis, we measured the expression of CD68 in GFP+ iMGs, which is representative of the size of the lysosomal compartment and indicative of the level of phagocytic activity in microglia (44). Quantification of the degree of colocalization of GFP and CD68 revealed a significant increase in CD68 in LPS-stimulated iMGs compared with unstimulated iMGs (Fig. 5 *C* and *D*, *Top*). Similar results were obtained for mouse microglia in the same chimeric brains (Fig. 5 *C* and *D*, *Bottom*). Thus, transplanted iMGs represent a potential model for studying activation of human microglia in the brain.

Discussion

The derivation of microglia-like cells from hiPSCs represents an important step for studying the role of microglia in neural development and neurodegenerative disease (18–20). However, there are important limitations to studying these cells in vitro, as primary microglia directly isolated from the brain exhibit significant changes in the expression of microglial signature genes and neurodegenerative disease-associated genes when grown in culture (26, 27). These findings suggested that in vitro differentiated microglia display a significantly altered phenotype and gene expression profile, thus limiting the use of such cells for disease research. The goal of this work was to overcome these limitations and establish an experimental platform that creates cells with a similar phenotype as primary human microglia. Microglial precursors were derived from hiPSCs and transplanted into the brains of neonatal mice. The injected microglial precursor cells displayed a developmental progression from immature microglia at 10 d after transplantation to a mature microglial phenotype at 60 and 120 d after transplantation that was similar to that of resting primary human microglia. The cells assumed a ramified morphology and robustly expressed microglia signature genes such as *P2RY12* and *TMEM119* that were weakly expressed in iMGs differentiated using in vitro protocols. Single-cell RNA-seq revealed that the transplanted cells resembled healthy primary microglia, while in vitro differentiated iMGs resembled primary microglia in a disease state (38). Finally, challenging the chimeric mice with LPS converted the resting human microglia into a typical activated state. Our

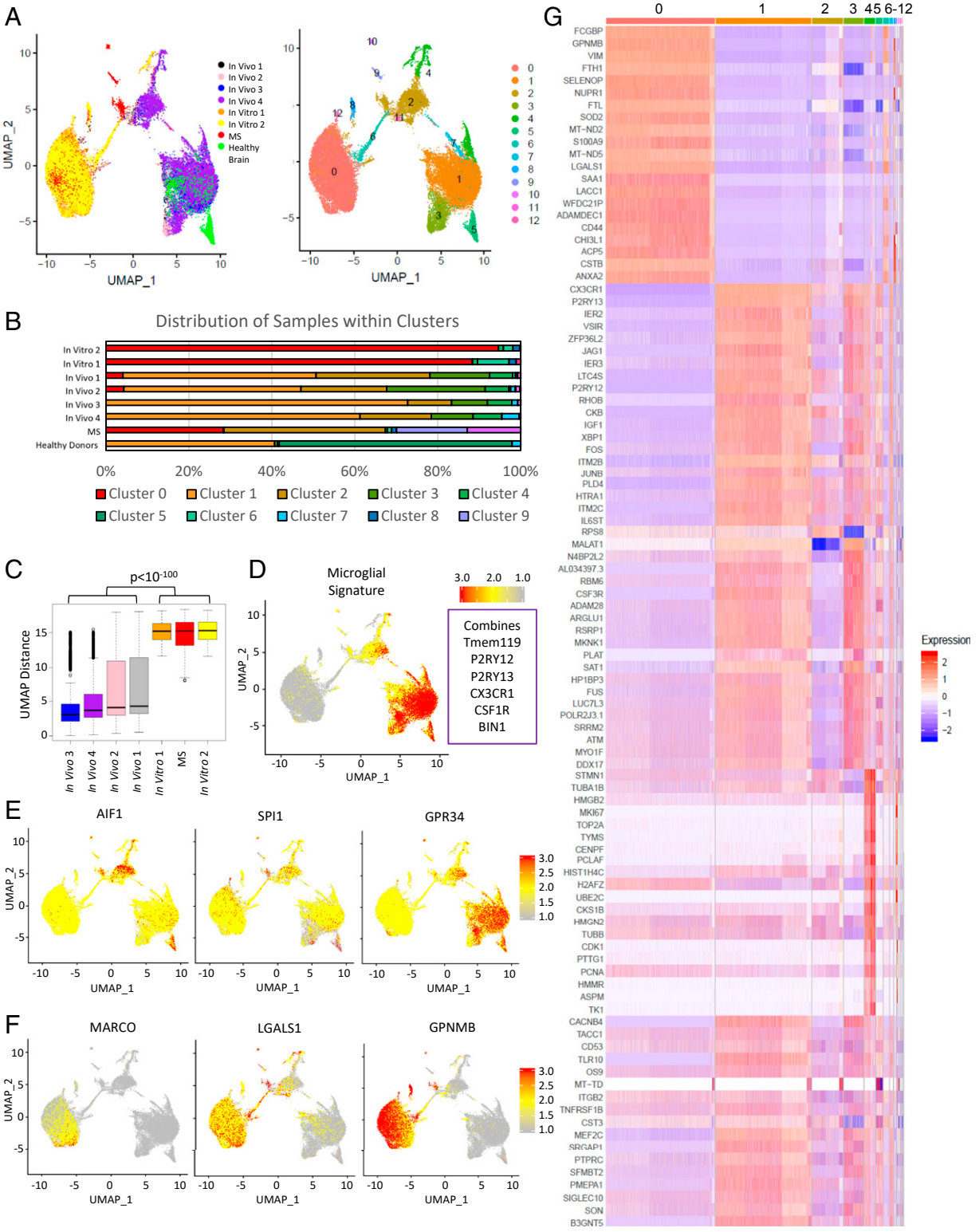

Fig. 4. Single-cell RNA-seq of 60-dpi in vivo and in vitro iMGs reveals similarities to primary human microglia in health and disease. (*A*) UMAP plots show clustering of 60-dpi in vivo iMGs and 60-d in vitro iMGs, as well as primary microglia from healthy donors and multiple sclerosis patients (38). Cells are colored by sample (*Left*) and by cluster (*Right*). (*B*) Graph showing the distribution of individual cells from each sample across the 13 clusters. (*C*) Boxplot showing the distance on the UMAP plot between each cell of a sample and the center of all cells in the healthy primary microglia sample. A Scheffé test showed that transplanted iMG samples are significantly closer to the healthy primary microglia ($P < 10^{-100}$) than other samples. (*D*) UMAP plot is colored according to a microglial signature score which combined normalized counts of *TMEM119*, *P2RY12*, *P2RY13*, *CX3CR1*, *CSF1R*, and *BIN1*. (*D*, *Upper Right*) Scale. (*E*) UMAP plots were colored according to the expression of myeloid-associated genes *AIF1*, *SPI1*, and *GPR34*. (*E*, *Right*) The scale correlates the natural log of the normalized counts to color. (*F*) UMAP plots are colored according to the expression of *LGALS1*, *GPMNB*, and *MARCO*. (*G*) Heatmap showing the 40 most differentially expressed genes in the 5 largest clusters.

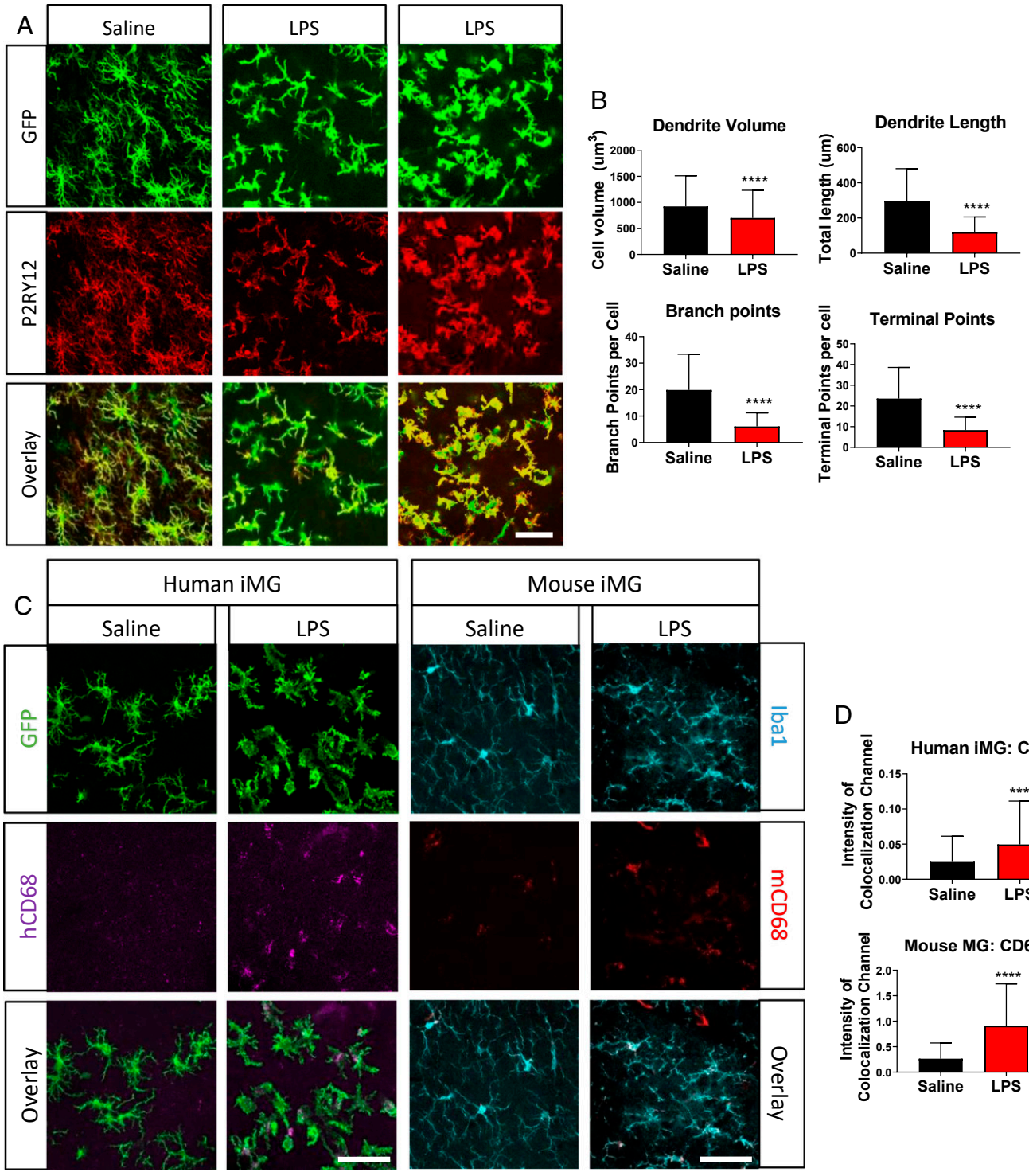

Fig. 5. iMGs in human–mouse microglial chimeras respond to LPS stimulation. (*A*) Representative images of 60-dpi iMGs following injection of saline (*Left*) or LPS (*Right*). Examples of moderate (*Middle*) and severe (*Right*) changes in morphology of GFP+ iMGs are shown from 2 separate mice. Cells are stained for GFP (green) and P2RY12 (red). (Scale bar, 50 μm.) (*B*) From the filament tracings, the total length of all summed processes per cell (dendrite length), total cell volume (dendrite volume), total number of bifurcation points per cell (branch points), and total number of process terminal points per cell (terminal points) in chimeras challenged with LPS or saline were quantified. (*C*) Representative images of CD68 staining in human 60-dpi iMGs in saline- and LPS-treated chimeras (*Left*) and mouse microglia from the same animals (*Right*). (Scale bar, 50 μm.) (*D*) The intensity of colocalization between GFP and human CD68 was quantified for human iMGs (*Top*) and the colocalization between Iba1 and mouse CD68 was quantified for mouse MGs (*Bottom*). Values are expressed as mean ± SD. Significance was determined by Mann–Whitney *t* test, with sample sizes of 150 to 300 cells from 3 mice. ****$P < 0.001$.

results indicate that the in vivo brain environment induces the microglia-like cells to a state similar to that of primary resting microglia.

To achieve efficient integration of donor microglia-like cells, 2 experimental parameters were crucial. First, the time of differentiation of donor cells in culture significantly impacted cell

integration. The most efficient integration of donor cells was achieved when iMPs were injected directly into neonatal brains without first differentiating cells into microglia-like cells. Second, the survival and integration of donor cells required the expression of human cytokines in the host animals. The recipient humanized NSG mice with the greatest number of integrated cells expressed the human versions of *CSF1*, *IL3*, *SCF*, and *GM-CSF*, with *CSF1* being the most important factor for donor cell integration. Under optimal experimental conditions, the donor cells attained up to 50% of the total number of microglia in some brain areas. We did not detect evidence of human cells replacing the host cells, as is seen when human astrocytes are injected into the newborn mouse brain (45).

The most important conclusion from our work is that the in vivo brain environment induces the transplanted microglia-like cells to assume a highly ramified phenotype with long processes seemingly surveying and contacting neurons as seen in the normal brain (1). Furthermore, our results show that in vivo differentiated iMGs are more similar to primary microglia than in vitro differentiated iMGs. Using both bulk and single-cell RNA-seq, we show that transplanted iMGs exhibit gene expression profiles much more similar to primary microglia than in vitro differentiated iMGs. This included significantly higher levels of expression of the key microglia signature genes *P2RY12*, *CX3CR1*, *P2RY13*, *SALL1*, and *BIN1* in transplanted iMGs. Furthermore, Alzheimer's and Parkinson's disease risk genes such as *GPNMB*, *ANXA1*, and *APOC1* were significantly upregulated in cultured iMGs. Finally, single-cell RNA-seq revealed that the transplanted microglia displayed cellular heterogeneity similar to that seen in healthy primary microglia in the human brain, while in vitro differentiated iMGs resembled primary microglia in a disease state (38). Thus, in vitro differentiated microglia do not well reflect the morphology and gene expression of microglia residing in the brain, confounding their use for disease research.

P2RY12, one of 2 microglial specific genes (46), was expressed in 95% of microglial precursors prior to injection but only in 40% of 10-dpi iMGs in chimeras. This could be due to a decrease in *P2RY12* during early stages of microglial maturation, as observed during in vitro differentiation in both protein and mRNA (*SI Appendix*, Fig. S1). Furthermore, the sensitivity of detecting P2RY12 by live-cell FACS is likely greater than the sensitivity of detection through immunostaining of fixed cells, which would further explain the differences in detection of P2RY12 between 10-d chimera iMGs and 10-d in vitro iMGs.

These results have recently been validated by a similar study which was published while this manuscript was in preparation (47). Using an alternative microglial differentiation protocol, this study confirmed that, through intraventricular injections of hematopoietic precursors into mice carrying a human allele of *CSF1*, transplanted iMGs are more similar to primary human cells than in vitro differentiated iMGs. As these 2 studies used different in vitro protocols to generate precursor cells yet reached similar conclusions (*SI Appendix*, Fig. S7), these results show that chimeras represent a robust strategy for minimizing the variability between protocols and between research groups which confounds in vitro research using hiPSC-derived microglial cells.

Microglia are known to become activated in response to immune stimulation, which is one of their primary functional roles (4, 5, 30, 40, 48). We show that the transplanted microglia strongly responded to LPS injection into the chimeras. Microglia underwent a phenotypic conversion from the ramified, resting state to an activated state, a response that is well-documented and associated with a characteristic shortening and thickening of processes as the cells acquire an amoeboid structure (36, 49, 50). Thus, the transplanted microglia react to signals in their environment in a way that is characteristic of primary microglia, further supporting the conclusion that they functionally integrate into and interact with the in vivo environment.

A major limitation of current protocols for the in vitro differentiation of microglia from hiPSCs has been the failure to define the "ground state" of the cells corresponding to resting-state microglia. Our work establishes an experimental platform that allows conversion of hiPSC-derived microglia-like cells to a state that closely resembles that of primary human microglia. Thus, relevant disease mutations can be introduced into the hiPSCs, allowing researchers to assess the phenotypic consequences on the ground state of the cells. This platform will allow future experiments to stringently test the role of Alzheimer's and Parkinson's disease risk alleles in neurodegenerative diseases.

Materials and Methods

A detailed description of experimental procedures and analyses is provided in *SI Appendix, Experimental Procedures*. Briefly, we transplanted microglial precursors derived from hiPSCs into the brains of NSG mice carrying the human allele for CSF1. These engrafted cells were then isolated for bulk RNA-seq and scRNA-seq and compared with in vitro differentiated cells and primary human microglia from published datasets in refs. 27 and 38, respectively. Animals were used in accordance with protocols approved by the Animal Research Regulation Committee at the Whitehead Institute and guidelines from the Department of Comparative Medicine at the Massachusetts Institute of Technology.

Data Availability. Single-cell and bulk RNA-sequencing data are available in the Gene Expression Omnibus (accession no. GSE139194). For further questions, please contact the corresponding author.

ACKNOWLEDGMENTS. We thank Patti Wisniewski, Hanna Aharonov, and Patrick Autissier for FACS, and Jennifer Love, Stephen Mraz III, Amanda Chilaka, and Sumeet Gupta for RNA-seq library preparation and sequencing. We thank Jesse Drotar, Stella Markoulaki, and Ruth Flannery for help with colony maintenance, and Beth Crimini for assisting with Cell Profiler. Finally, we thank Marine Krzisch, Micheal Gallagher, Raaji Alagappan, Shawn Lui, Haiting Ma, Tenzin Lungjangwa, Alexsia Richards, Carrie Garrett-Engele, Yuelin Song, Malkiel Cohen, Emile Wogram, and Frank Soldner for reagents, technical assistance, and input. This work was supported by the Cure Alzheimer's Foundation, MassCATS, and NIH Grants R01 AG058002-01, R01 MH104610, R37 CA084198, and U19 AI131135 (to R.J.). L.D.S. is supported by NIH Grants R24 OD26440, AI32963, and CA034196. J.S. is supported by the National Institute of Child Health and Human Development (K99HD096049).

1. A. Nimmerjahn, F. Kirchhoff, F. Helmchen, Resting microglial cells are highly dynamic surveillants of brain parenchyma in vivo. *Science* **308**, 1314–1318 (2005).
2. D. P. Schafer *et al.*, Microglia sculpt postnatal neural circuits in an activity and complement-dependent manner. *Neuron* **74**, 691–705 (2012).
3. T. Bolmont *et al.*, Dynamics of the microglial/amyloid interaction indicate a role in plaque maintenance. *J. Neurosci.* **28**, 4283–4292 (2008).
4. A. Majumdar *et al.*, Activation of microglia acidifies lysosomes and leads to degradation of Alzheimer amyloid fibrils. *Mol. Biol. Cell* **18**, 1490–1496 (2007).
5. M. W. Salter, B. Stevens, Microglia emerge as central players in brain disease. *Nat. Med.* **23**, 1018–1027 (2017).
6. S. R. Subramaniam, H. J. Federoff, Targeting microglial activation states as a therapeutic avenue in Parkinson's disease. *Front. Aging Neurosci.* **9**, 176 (2017).
7. L. Du *et al.*, Role of microglia in neurological disorders and their potentials as a therapeutic target. *Mol. Neurobiol.* **54**, 7567–7584 (2017).
8. H. Mathys *et al.*, Temporal tracking of microglia activation in neurodegeneration at single-cell resolution. *Cell Rep.* **21**, 366–380 (2017).
9. M. Olah *et al.*, A transcriptomic atlas of aged human microglia. *Nat. Commun.* **9**, 539 (2018).
10. Z. Yin *et al.*, Immune hyperreactivity of Aβ plaque-associated microglia in Alzheimer's disease. *Neurobiol. Aging* **55**, 115–122 (2017).
11. P. L. McGeer, S. Itagaki, H. Tago, E. G. McGeer, Reactive microglia in patients with senile dementia of the Alzheimer type are positive for the histocompatibility glycoprotein HLA-DR. *Neurosci. Lett.* **79**, 195–200 (1987).
12. D. Chang *et al.*; International Parkinson's Disease Genomics Consortium; 23andMe Research Team, A meta-analysis of genome-wide association studies identifies 17 new Parkinson's disease risk loci. *Nat. Genet.* **49**, 1511–1516 (2017).
13. D. Harold *et al.*, Genome-wide association study identifies variants at CLU and PICALM associated with Alzheimer's disease. *Nat. Genet.* **41**, 1088–1093 (2009). Errata in: *Nat. Genet.* **41**, 1156 (2009) and **45**, 712 (2013).

14. P. Hollingworth *et al.*; Alzheimer's Disease Neuroimaging Initiative; CHARGE Consortium; EADI1 Consortium, Common variants at ABCA7, MS4A6A/MS4A4E, EPHA1, CD33 and CD2AP are associated with Alzheimer's disease. *Nat. Genet.* **43**, 429–435 (2011).
15. J. C. Lambert *et al.*; European Alzheimer's Disease Initiative (EADI); Genetic and Environmental Risk in Alzheimer's Disease; Alzheimer's Disease Genetic Consortium; Cohorts for Heart and Aging Research in Genomic Epidemiology, Meta-analysis of 74,046 individuals identifies 11 new susceptibility loci for Alzheimer's disease. *Nat. Genet.* **45**, 1452–1458 (2013).
16. A. C. Naj *et al.*, Common variants at MS4A4/MS4A6E, CD2AP, CD33 and EPHA1 are associated with late-onset Alzheimer's disease. *Nat. Genet.* **43**, 436–441 (2011).
17. L. Bertram *et al.*, Genome-wide association analysis reveals putative Alzheimer's disease susceptibility loci in addition to APOE. *Am. J. Hum. Genet.* **83**, 623–632 (2008).
18. E. M. Abud *et al.*, iPSC-derived human microglia-like cells to study neurological diseases. *Neuron* **94**, 278–293.e9 (2017).
19. P. Douvaras *et al.*, Directed differentiation of human pluripotent stem cells to microglia. *Stem Cell Rep.* **8**, 1516–1524 (2017).
20. H. Pandya *et al.*, Differentiation of human and murine induced pluripotent stem cells to microglia-like cells. *Nat. Neurosci.* **20**, 753–759 (2017).
21. J. Muffat *et al.*, Efficient derivation of microglia-like cells from human pluripotent stem cells. *Nat. Med.* **22**, 1358–1367 (2016).
22. W. Haenseler *et al.*, A highly efficient human pluripotent stem cell microglia model displays a neuronal-co-culture-specific expression profile and inflammatory response. *Stem Cell Rep.* **8**, 1727–1742 (2017).
23. K. Takata *et al.*, Induced-pluripotent-stem-cell-derived primitive macrophages provide a platform for modeling tissue-resident macrophage differentiation and function. *Immunity* **47**, 183–198.e6 (2017).
24. Y. Wang *et al.*, IL-34 is a tissue-restricted ligand of CSF1R required for the development of Langerhans cells and microglia. *Nat. Immunol.* **13**, 753–760 (2012).
25. B. Erblich, L. Zhu, A. M. Etgen, K. Dobrenis, J. W. Pollard, Absence of colony stimulation factor-1 receptor results in loss of microglia, disrupted brain development and olfactory deficits. *PLoS One* **6**, e26317 (2011).
26. C. J. Bohlen *et al.*, Diverse requirements for microglial survival, specification, and function revealed by defined-medium cultures. *Neuron* **94**, 759–773.e8 (2017).
27. D. Gosselin *et al.*, An environment-dependent transcriptional network specifies human microglia identity. *Science* **356**, eaal3222 (2017).
28. M. D. Yanagimachi *et al.*, Robust and highly-efficient differentiation of functional monocytic cells from human pluripotent stem cells under serum- and feeder cell-free conditions. *PLoS One* **8**, e59243 (2013).
29. H. Lin *et al.*, Discovery of a cytokine and its receptor by functional screening of the extracellular proteome. *Science* **320**, 807–811 (2008).
30. F. Ginhoux, M. Prinz, Origin of microglia: Current concepts and past controversies. *Cold Spring Harb. Perspect. Biol.* **7**, a020537 (2015).
31. R. Ito *et al.*, Establishment of a human allergy model using human IL-3/GM-CSF-transgenic NOG mice. *J. Immunol.* **191**, 2890–2899 (2013).
32. M. Wunderlich *et al.*, AML xenograft efficiency is significantly improved in NOD/SCID-IL2RG mice constitutively expressing human SCF, GM-CSF and IL-3. *Leukemia* **24**, 1785–1788 (2010).
33. J. K. Skelton, A. M. Ortega-Prieto, M. Dorner, A hitchhiker's guide to humanized mice: New pathways to studying viral infections. *Immunology* **154**, 50–61 (2018).
34. M. A. Cohen, S. Markoulaki, R. Jaenisch, Matched developmental timing of donor cells with the host is crucial for chimera formation. *Stem Cell Rep.* **10**, 1445–1452 (2018).
35. V. L. Mascetti, R. A. Pedersen, Human-mouse chimerism validates human stem cell pluripotency. *Cell Stem Cell* **18**, 67–72 (2016).
36. M. L. Bennett *et al.*, New tools for studying microglia in the mouse and human CNS. *Proc. Natl. Acad. Sci. U.S.A.* **113**, E1738–E1746 (2016).
37. T. Mizuno *et al.*, Interleukin-34 selectively enhances the neuroprotective effects of microglia to attenuate oligomeric amyloid-β neurotoxicity. *Am. J. Pathol.* **179**, 2016–2027 (2011).
38. T. Masuda *et al.*, Spatial and temporal heterogeneity of mouse and human microglia at single-cell resolution. *Nature* **566**, 388–392 (2019).
39. H. Keren-Shaul *et al.*, A unique microglia type associated with restricting development of Alzheimer's disease. *Cell* **169**, 1276–1290.e17 (2017).
40. I. C. Hoogland, C. Houbolt, D. J. van Westerloo, W. A. van Gool, D. van de Beek, Systemic inflammation and microglial activation: Systematic review of animal experiments. *J. Neuroinflammation* **12**, 114 (2015).
41. D. M. Norden, P. J. Trojanowski, E. Villanueva, E. Navarro, J. P. Godbout, Sequential activation of microglia and astrocyte cytokine expression precedes increased Iba-1 or GFAP immunoreactivity following systemic immune challenge. *Glia* **64**, 300–316 (2016).
42. M. Fricker, M. J. Oliva-Martín, G. C. Brown, Primary phagocytosis of viable neurons by microglia activated with LPS or Aβ is dependent on calreticulin/LRP phagocytic signalling. *J. Neuroinflammation* **9**, 196 (2012).
43. J. J. Neher *et al.*, Inhibition of microglial phagocytosis is sufficient to prevent inflammatory neuronal death. *J. Immunol.* **186**, 4973–4983 (2011).
44. C. Perego, S. Fumagalli, M. G. De Simoni, Temporal pattern of expression and colocalization of microglia/macrophage phenotype markers following brain ischemic injury in mice. *J. Neuroinflammation* **8**, 174 (2011).
45. M. S. Windrem *et al.*, Human iPSC glial mouse chimeras reveal glial contributions to schizophrenia. *Cell Stem Cell* **21**, 195–208.e6 (2017).
46. U. B. Eyo *et al.*, P2Y12R-dependent translocation mechanisms gate the changing microglial landscape. *Cell Rep.* **23**, 959–966 (2018).
47. J. Hasselmann *et al.*, Development of a chimeric model to study and manipulate human microglia in vivo. *Neuron* **103**, 1016–1033.e10 (2019).
48. C. Sousa *et al.*, Single-cell transcriptomics reveals distinct inflammation-induced microglia signatures. *EMBO Rep.* **19**, e46171 (2018).
49. D. J. Hines, H. B. Choi, R. M. Hines, A. G. Phillips, B. A. MacVicar, Prevention of LPS-induced microglia activation, cytokine production and sickness behavior with TLR4 receptor interfering peptides. *PLoS One* **8**, e60388 (2013).
50. S. Kondo, S. Kohsaka, S. Okabe, Long-term changes of spine dynamics and microglia after transient peripheral immune response triggered by LPS in vivo. *Mol. Brain* **4**, 27 (2011).